Journal of Fluids and Structures 21 (2005) 769–778

JOURNAL OF FLUIDS AND STRUCTURES

www.elsevier.com/locate/jfs

On the Rayleigh conductivity of a bias-flow aperture

T. Luong[a], M.S. Howe[a,*], R.S. McGowan[b]

[a]Boston University, College of Engineering, 110 Cummington Street, Boston, MA 02215, USA
[b]CReSS LLC, 1 Seaborn Place, Lexington, MA 02420, USA

Received 31 May 2005; accepted 7 September 2005
Available online 25 October 2005

Abstract

An analysis is made of the attenuation of sound by vorticity production in a bias flow aperture. A modified form of the Cummings equation describing unsteady flow through a small aperture is used to extend the linear theory of the bias flow conductivity of a circular aperture in a thin wall of Howe (1979. On the theory of unsteady high Reynolds number flow through a circular aperture. Proceedings of the Royal Society of London A 366, 205–233) to a wall of arbitrary thickness and to examine the influence acoustic nonlinearity within the aperture. Numerical results are compared with existing analytic predictions of linear theory. It is shown that attenuations predicted by both linear and nonlinear theories agree over a wide range of incident acoustic pressures, approaching in amplitude that required to maintain the steady mean flow through the aperture. The dominant nonlinear effect is a small reduction (less than about 5%) in the mean bias flow velocity. Application of the Cummings equation in the linear regime leads to a new, simple formula for the bias flow conductivity for a screen of finite thickness.

1. Introduction

Vorticity is produced by fluid motion over a solid surface, the rate of production being greatest in regions where the pressure and velocity in the primary flow change rapidly, such as at corners and sharp edges. The kinetic energy of the vortex motion is derived from the primary flow, and when this is a sound wave incident, for example, on a sharp edge, vorticity diffuses from the edge and causes the sound to be damped. For a nominally stationary fluid the dissipation of sound is caused by the nonlinear convection of vorticity from the edge and its subsequent viscous damping, both of which are generally weak (Zinn, 1970; Melling, 1973; Cummings, 1984). The damping is significantly increased, however, in the presence of mean flow (Dean and Tester, 1975; Bechert et al., 1977; Howe, 1979,1980,1998; Ver, 1982,1990; Hughes and Dowling, 1990; Dowling and Hughes, 1992; Dupere and Dowling, 2000; Eldredge and Dowling, 2003). In many applications the flows are at sufficiently high Reynolds numbers that viscosity is important only very close to the boundary at which the vorticity is produced; the shed vorticity is swept away by the mean flow, and its kinetic energy is permanently lost to the sound.

The damping is easily quantified at low Mach numbers, when locally the effects of compressibility on the shed vorticity are not important. Then the rate Π of dissipation of acoustic energy can be expressed as an integral

*Corresponding author. Tel.: +1 617 484 0656; fax: +1 617 353 5866.
E-mail address: mshowe@bu.edu (M.S. Howe).

0889-9746/$ - see front matter
doi:10.1016/j.jfluidstructs.2005.09.010

of the form (Howe, 1980,1998)

$$\Pi \approx \rho_o \int \boldsymbol{\omega} \wedge \mathbf{v} \cdot \mathbf{u} \, \mathrm{d}^3\mathbf{x}, \tag{1.1}$$

where ρ_o is the mean density, $\mathbf{v}$ the velocity, $\boldsymbol{\omega}$ the vorticity, and $\mathbf{u}$ is the acoustic particle velocity. In the absence of mean flow a sound wave of amplitude ε incident on an edge will produce shed vorticity $\boldsymbol{\omega}$ and local velocity fluctuations $\mathbf{v}$ both of order ε, so that this equation implies that the damping Π is relatively weak, being third order ($\sim\mathcal{O}(\varepsilon^3)$) in the acoustic amplitude.

When, however, there exists an independent and substantial mean flow both $\mathbf{v}$ and the vorticity $\boldsymbol{\omega}$ can have large mean components that are independent of the incident sound. In this case the time-dependent part of $\boldsymbol{\omega} \wedge \mathbf{v} \sim \mathcal{O}(\varepsilon)$, so that the time averaged dissipation predicted by (1.1) is formally increased by an order of magnitude to $\Pi \sim \mathcal{O}(\varepsilon^2)$. This is the theoretical explanation of the enhanced damping achieved by a bias flow perforated screen of the type illustrated schematically in Fig. 1. A nominally steady, low Mach number mean flow through the screen (conveyed by the bias flow 'jets' in the apertures) is maintained by application of a steady pressure load. When the Reynolds number (based on aperture diameter) is large, the flow through an aperture is uninfluenced by viscosity except near the aperture edge,

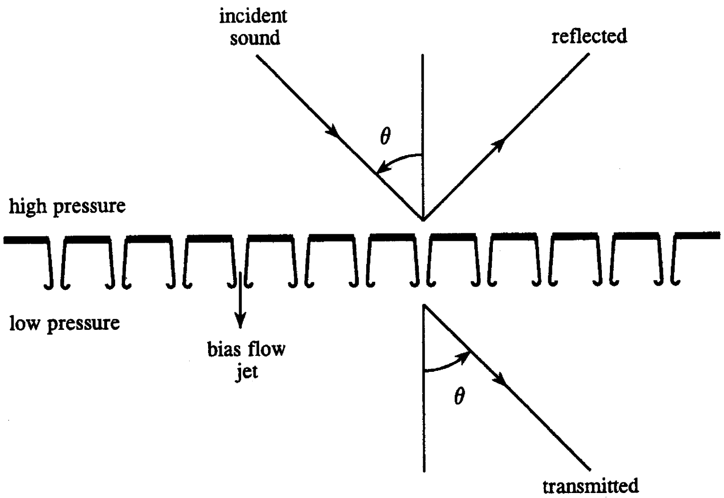

Figure 1. Schematic bias flow perforated screen.

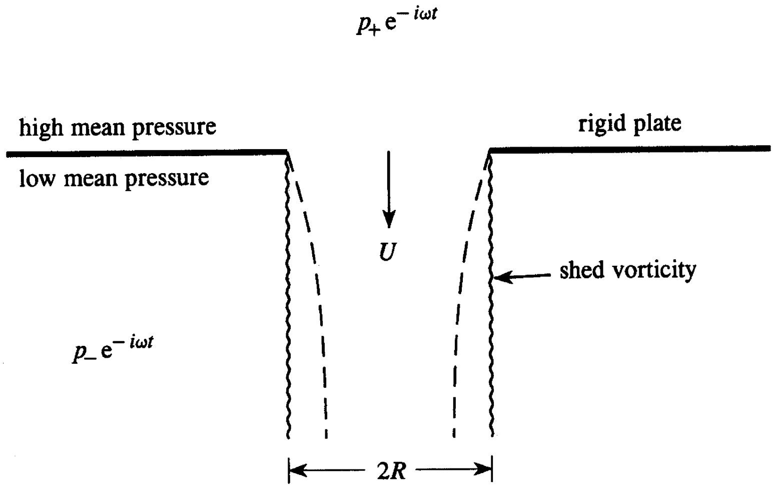

Figure 2. Linearized model of sound interacting with a bias flow jet.

where the flow separates to form a jet. Vorticity generated at the edge by incident sound is swept away in the jet, and damping occurs by the transfer of acoustic energy to the kinetic energy of the jet.

The *linear* theory of dissipation in a bias flow jet (Howe, 1979,1998) is based on the model of Fig. 2, involving an acoustically compact circular aperture of radius R in a rigid wall of negligible thickness, and is briefly reviewed in Section 2 of this paper. Predictions of this linear theory applied to damping by bias flow perforated screens have shown good agreement with experiment (Ver, 1982,1990; Hughes and Dowling, 1990; Eldredge and Dowling, 2003). There are many applications, however, where the amplitude of the pressure loading $p_+ - p_-$ is large and comparable with the mean pressure drop across the screen responsible for the bias flow. Such cases are not strictly covered by the linear theory, and one purpose of this paper is to consider an extension of the theory to large acoustic amplitudes. Special cases of this problem have been discussed by Jing and Sun (2002) using an approximate numerical treatment based on the 'vortex blob method', with particular attention to situations where the acoustic amplitude is large enough to produce mean flow reversal. In the present paper, however, interest is restricted to situations where the acoustic amplitude is large, but not large enough to induce reversal of the mean flow. This is the case of most practical importance. Our new approach is based on a modified form of Cummings' (1984,1986) empirical equation for unsteady flow through an aperture subject to unsteady pressure loading. It can also be used to extend the elementary thin wall theory of Howe (1979,1998) to account for finite wall thickness. These applications of the Cummings equation are discussed in Sections 3 and 4, and the results are used (Section 5) to derive a simple general formula for the bias flow conductivity for an aperture in a thick wall.

2. Linear theory for a thin wall

The mean jet velocity in the plane of the aperture in Fig. 2 is denoted by U. It is modulated by a locally uniform time-harmonic pressure differential equal to the real part of $(p_+ - p_-)\mathrm{e}^{-\mathrm{i}\omega t}$. The motion near the aperture can be regarded as incompressible, with unsteady volume flux $Q\mathrm{e}^{-\mathrm{i}\omega t}$ through the aperture (from 'above' to 'below' the plate in Fig. 2). The acoustic properties of the bias flow jet are then determined by the *Rayleigh conductivity* K_R defined by (Howe, 1998; Rayleigh, 1945)

$$K_R = \frac{-\mathrm{i}\omega\rho_o Q}{(p_+ - p_-)}. \tag{2.1}$$

An approximate formula for K_R is known (Howe, 1979,1998) for an aperture in a *thin* wall when U is small compared to the speed of sound. An ideal jet actually contracts to an asymptotic diameter equal to about 0.62 times that of the aperture, in the manner indicated by the dashed profile in the figure (Lamb, 1932; Birkhoff and Zarantonello, 1957); when the flow is turbulent, however, turbulence diffusion will tend to produce an expanding flow. In the linearized approximation the fluctuations in the flow produced by the unsteady pressure differential $p_+ - p_-$ are regarded as axisymmetric, and the additional vorticity generated at the edge of the aperture may be envisaged as a succession of vortex rings with infinitesimal cores, which convect at a velocity U_c and form an axisymmetric vortex sheet within the mean shear layer of the jet. Experiment (Hughes and Dowling, 1990; Dowling and Hughes, 1992) indicates that to a good approximation the convection velocity U_c may be set equal to the mean jet velocity U in the plane of the aperture. To calculate the conductivity the back reaction of these vortex rings on the aperture flow must be determined. This is easily done if the variation in the radius of a ring is neglected, so that the vortex sheet is cylindrical, and equal to the aperture radius R (as in Fig. 2), in which case it is found that (Howe, 1979,1998)

$$K_R = 2R(\Gamma - \mathrm{i}\Delta), \tag{2.2}$$

where the real and imaginary components Γ, Δ are determined by

$$\Gamma - \mathrm{i}\Delta = 1 + \frac{(\pi/2)\mathrm{I}_1(\kappa R)\mathrm{e}^{-\kappa R} - \mathrm{i}\mathrm{K}_1(\kappa R)\sinh(\kappa R)}{\kappa R[(\pi/2)\mathrm{I}_1(\kappa R)\mathrm{e}^{-\kappa R} + \mathrm{i}\mathrm{K}_1(\kappa R)\cosh(\kappa R)]}, \quad \kappa = \frac{\omega}{U} > 0, \tag{2.3}$$

where I_1, K_1 are modified Bessel functions. The functions Γ and Δ are shown plotted against the Strouhal number $\omega R/U$ in Fig. 3.

At very high frequencies ($\Gamma \sim 1$, $\Delta \sim 0$) vorticity production by the sound has a negligible influence on the flow because the length scale of the unsteady vorticity $\sim U/\omega$ is small and velocities induced by successive elementary vortex rings largely cancel; the conductivity then reverts to its value $K_R = 2R$ in the absence of the jet. On the other hand, when $\omega R/U \to 0$, unsteady vorticity of one sign can stretch many aperture diameters downstream and produce a strong effect on the flow.

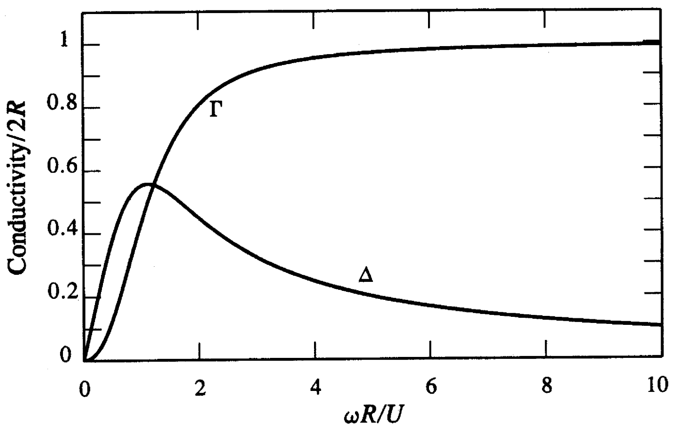

Figure 3. Linear theory conductivity of a bias flow circular aperture.

Because the local motion at the aperture is approximated as incompressible, the power Π extracted from the oscillating pressure load $p_+ - p_-$ to produce vorticity is just equal to $\langle \mathscr{Re}(Q\mathrm{e}^{-\mathrm{i}\omega t})\mathscr{Re}([p_+ - p_-]e^{-\mathrm{i}\omega t})\rangle$, where the angle brackets denote a time average, and the real parts of the fluctuating quantities are to be taken. Using Eqs. (2.1) and (2.2), we find

$$\Pi = \tfrac{1}{4}([p_+ - p_-]^* Q + [p_+ - p_-]Q^*)$$
$$= \frac{|p_+ - p_-|^2 R\Delta}{\rho_o \omega}, \tag{2.4}$$

which is positive definite for all real frequencies.

The linearized theory leading to Eq. (2.3) is not strictly applicable to apertures in a wall of finite thickness ℓ_w, say. In that case the definition (2.2) is written

$$K_R = K_o(\Gamma - \mathrm{i}\Delta), \tag{2.5}$$

where K_o is the conductivity in the absence of the bias flow, given approximately by

$$K_o = \frac{A}{2\ell_o + \ell_w}, \quad \left(\ell_o = \frac{\pi R}{4}, \quad A = \pi R^2\right). \tag{2.6}$$

Explicit approximations for Γ and Δ when $\ell_w > 0$ are discussed in Section 5.

3. The Cummings equation applied to a bias flow aperture

Consider a circular aperture in a rigid plate (as in Fig. 2) when the plate has finite thickness ℓ_w. Let the mean flow in the absence of sound be produced by a pressure drop p_o across the plate. In terms of the 'contraction ratio' σ of the jet, the mean velocity U in the entrance plane of the aperture is determined by the steady form of Bernoulli's equation

$$\frac{U^2}{2\sigma^2} = \frac{p_o}{\rho_o}. \tag{3.1}$$

In the presence of sound, choose the time origin so that the applied time-harmonic pressure loading can be taken in the form

$$p_I \cos(\omega t) = \mathscr{Re}\{(p_+ - p_-)\mathrm{e}^{-\mathrm{i}\omega t}\}, \tag{3.2}$$

where $p_I > 0$. Let $V(t)$ be the corresponding change in U produced by the additional pressure $p_I \cos(\omega t)$, so that the jet velocity averaged over the plane of the aperture is $U + V(t)$. Then the Cummings empirical equation (Cummings, 1984,1986) assumes the following form when expressed in terms of $V(t)$:

$$\bar{\ell}(t)\frac{\mathrm{d}V}{\mathrm{d}t}+\frac{1}{2\sigma^2}(U+V)|U+V|=\frac{p_o+p_I\ \cos(\omega t)}{\rho_o}. \tag{3.3}$$

This describes the motion of a slug of fluid of variable effective length $\bar{\ell}(t)$ and variable mass $\rho_o A\bar{\ell}(t)$ (where $A=\pi R^2$ is the area of the aperture) subject to an excess driving pressure $p_o+p_I\ \cos(\omega t)$ and a resistive force $-(1/2\sigma^2)\rho_o A(U+V)|U+V|$.

If the flow were entirely irrotational (no jet formation) the length $\bar{\ell}(t)$ would be constant and equal approximately to $2\ell_o+\ell_w$, where $\ell_o\approx(\pi/4)R$ is the 'end-correction' of the aperture opening into irrotational flow on *one* side of the plate (Howe, 1998; Rayleigh, 1945). When a jet is formed, however, Cummings argued that $\bar{\ell}(t)$ becomes a function of the effective length $\mathscr{L}$ of the jet defined by

$$\mathscr{L}(\tau)=\int_0^\tau |U+V(t)|\ \mathrm{d}t, \tag{3.4}$$

where the time τ is measured from the beginning of the acoustic half cycle during which the sign of $U+V(t)$ is constant. From an examination of data from several experiments, in which the working fluid was either water or air, Cummings (1986) proposed the following empirical relation between $\bar{\ell}(t)$ and $\mathscr{L}$:

$$\bar{\ell}(t)=\ell_o+\frac{\ell_w+\ell_o}{1+(\mathscr{L}/2R)^{1.585}/3}. \tag{3.5}$$

Thus, as the jet length $\mathscr{L}$ increases from zero, $\bar{\ell}$ decreases because the inertia of the ideal potential flow through the aperture and on the jet side of the plate is progressively replaced by that of the jet.

However, this formula must be modified when the jet length $\mathscr{L}$ is indefinitely large, which occurs when $p_I\leqslant p_o$, so that the net driving pressure $p_o+p_I\ \cos(\omega t)$ never changes sign. This is the case in typical bias flow applications to acoustics, even when the acoustic amplitude is large. Then the second term on the right of Eq. (3.5) rapidly decreases to zero and $\bar{\ell}(t)\to\ell_o$. This would imply that only the fluid inertia on one side of the aperture affects the motion through the aperture, whereas pulsational motions actually occur on both sides, even in the presence of the jet. Thus, whereas Cummings' formula (3.5) provides a good representation of the inertia fluctuations during jet formation, it ceases to be effective in the absence of flow reversal in the aperture. At high frequencies ($\omega R/U>1$, to the right of the dissipation peak in Fig. 3) pulsations in the momentum flux through the aperture cannot continue to be absorbed by acceleration of the incompressible jet, whose inertia becomes unbounded as $\mathscr{L}\to\infty$. In this case the unsteady volume flux through the aperture must cause pulsations in the jet cross-sectional area within and just downstream of the aperture, with little or no effect in the body of the jet. This produces an irrotational response in the exterior fluid that must be essentially similar to that in the absence of the jet. In these circumstances $\bar{\ell}$ must revert to its value $\bar{\ell}=2\ell_o+\ell_w$ for a jet-free aperture flow.

But, at low frequencies the changes in the jet can be regarded as quasi-static and the acceleration term on the left of Cummings' equation (3.3) becomes small. Then the applied pressure causes the jet kinetic energy to change slowly, the transfer mechanism being represented by the quadratic term on the left of (3.3). The transition between the high- and low-frequency responses of the jet is governed by the value of the effective contraction coefficient σ. According to Cummings (1986), the approximation $\sigma=0.75$ gives predictions that agree well with experiment. Our comparison below with the linear thin-wall theory will confirm this conclusion for the bias flow problem, and also support the hypothesis $\bar{\ell}=2\ell_o+\ell_w$ at higher frequencies.

4. Numerical results for nonlinear aperture flow

4.1. Modified bias flow equation

After this preliminary discussion of the Cummings equation, we now introduce the modified form suitable for studying bias flow oscillations. It will be assumed throughout that the mean bias flow pressure p_o is sufficiently in excess of the acoustic pressure load p_I across the plate to preclude flow reversal in the aperture. This implies that $|U+V|\equiv(U+V)$ in (3.3). Introducing this change in Eq. (3.3), subtracting Eq. (3.1), and putting $\bar{\ell}=2\ell_o+\ell_w$, results in the following modified Cummings equation:

$$(2\ell_o+\ell_w)\frac{\mathrm{d}V}{\mathrm{d}t}+\frac{V}{\sigma^2}\left(U+\frac{V}{2}\right)=\frac{p_I\ \cos(\omega t)}{\rho_o}, \tag{4.1}$$

where

$$\ell_o = \frac{\pi R}{4}, \quad \sigma = 0.75. \tag{4.2}$$

The steady-state velocity fluctuations forced by the time-harmonic applied pressure also have period $2\pi/\omega$ but are not necessarily sinusoidal, and we must put

$$V(t) = \mathscr{R}e \sum_{n=0}^{\infty} V_n \mathrm{e}^{-\mathrm{i}n\omega t}. \tag{4.3}$$

Fig. 4 illustrates the predicted influence of nonlinearity in the aperture for the three cases $p_I/\rho_o U^2 = 0.1, 0.5, 1.0$ at the three Strouhal numbers $\omega R/U = 0.25, 1, 2$ for an aperture in a thin wall ($\ell_w = 0$). The figure shows plots of $V(t)/U =$ nondimensional unsteady volume flux through the aperture, calculated by numerical integration of (4.1) starting at $t = 0$ with $V = 0$ and continuing until a steady state is established. The results indicate that nonlinearity becomes progressively important as the driving pressure amplitude increases principally at the lower frequencies $\omega R/U < 1$ (to the left of the linear theory damping peak in Fig. 3).

4.2. Comparison with linear theory

According to linear theory the unsteady volume flux is determined by the complex conductivity $K_R = K_o(\Gamma - \mathrm{i}\Delta)$, in terms of which Eq. (2.1) implies that

$$\Gamma = \frac{2\rho_o \omega}{K_o p_\mathrm{I}} \langle \mathscr{R}e(Q\mathrm{e}^{-\mathrm{i}\omega t}) \sin \omega t \rangle,$$
$$\Delta = \frac{2\rho_o \omega}{K_o p_\mathrm{I}} \langle \mathscr{R}e(Q\mathrm{e}^{-\mathrm{i}\omega t}) \cos \omega t \rangle. \tag{4.4}$$

In the nonlinear problem the linear theory volume flux $\mathscr{R}e(Q\mathrm{e}^{-\mathrm{i}\omega t})$ is replaced by $AV(t)$. We can formally perform the same calculation to determine the corresponding values of the frequency dependent coefficients Γ, Δ. This is equivalent

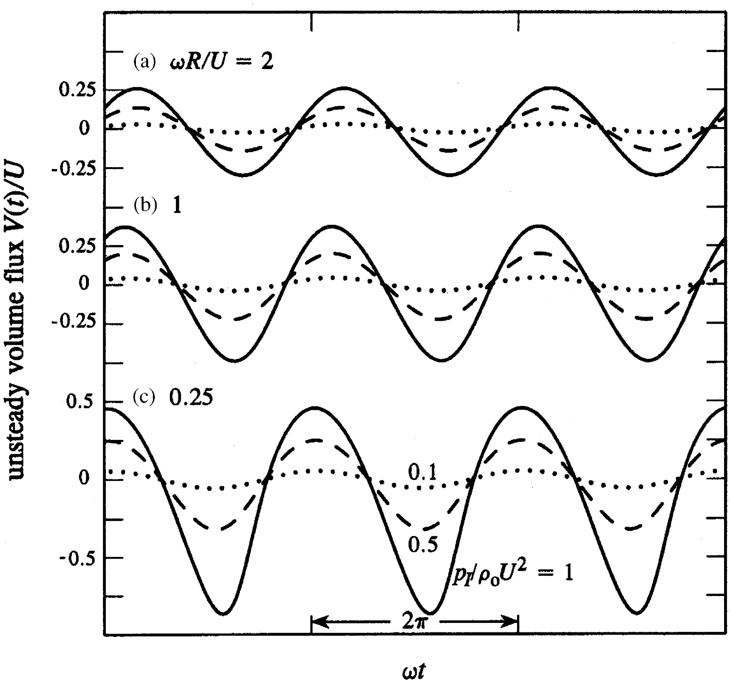

Figure 4. Typical plots of the unsteady volume flux through the aperture predicted by numerical integration of the Cummings equation (4.1).

to replacing $\mathscr{Re}(Q\mathrm{e}^{-\mathrm{i}\omega t})$ in (4.4) by $\mathscr{Re}(AV_1\mathrm{e}^{-\mathrm{i}\omega t})$; the calculation can also be performed directly using the numerical solution of Eq. (4.1), in terms of which

$$\Gamma = \frac{2\rho_o\omega A}{K_o p_I}\,\frac{\omega}{2\pi}\int_{t_o}^{t_o+2\pi/\omega} V(t)\,\sin(\omega t)\,\mathrm{d}t,$$
$$\Delta = \frac{2\rho_o\omega A}{K_o p_I}\,\frac{\omega}{2\pi}\int_{t_o}^{t_o+2\pi/\omega} V(t)\,\cos(\omega t)\,\mathrm{d}t, \tag{4.5}$$

where t_o is large enough for the steady-state solution to be fully established.

By evaluating these integrals for $p_I/\rho_o U^2 \ll 1$ predictions of the Cummings equation (4.1) can be compared with the linear theory of Section 2. To do this we must set $\ell_w = 0$ in (4.1), corresponding to $K_o = 2R$ for a circular aperture in a thin wall. In Fig. 5 the linear theory values of Γ and Δ (dotted curves: $\cdots$) are compared with predictions of (4.5) for the three cases $\sigma = 0.6, 0.75, 0.85$ when $p_I/\rho_o U^2 = 0.1$. It can be seen that the value $\sigma = 0.75$ recommended by Cummings (1986) yields excellent agreement with linear theory for Γ, and the closest agreement with linear theory for Δ.

At large Strouhal numbers $\omega R/U$, the terms in the expansion (4.3) decrease rapidly with n. This is not unexpected, because in this limit the left-hand side of Eq. (4.1) is dominated by the acceleration inertia term. The leading approximation to the solution when $\ell_w = 0$ is then easily shown to be the linear theory approximation

$$V(t) \approx \frac{2p_I}{\pi\rho_o\omega R}\left[\sin\omega t + \frac{2}{\pi\sigma^2(\omega R/U)}\cos\omega t\right], \quad \frac{\omega R}{U} \gg 1. \tag{4.6}$$

In this limit Eqs. (4.5) imply that

$$\Gamma \approx 1, \quad \Delta \approx \frac{2}{\pi\sigma^2(\omega R/U)}.$$

The corresponding asymptotic values obtained from the linear theory formula (2.3) are

$$\Gamma \approx 1, \quad \Delta \approx \frac{1}{(\omega R/U)}.$$

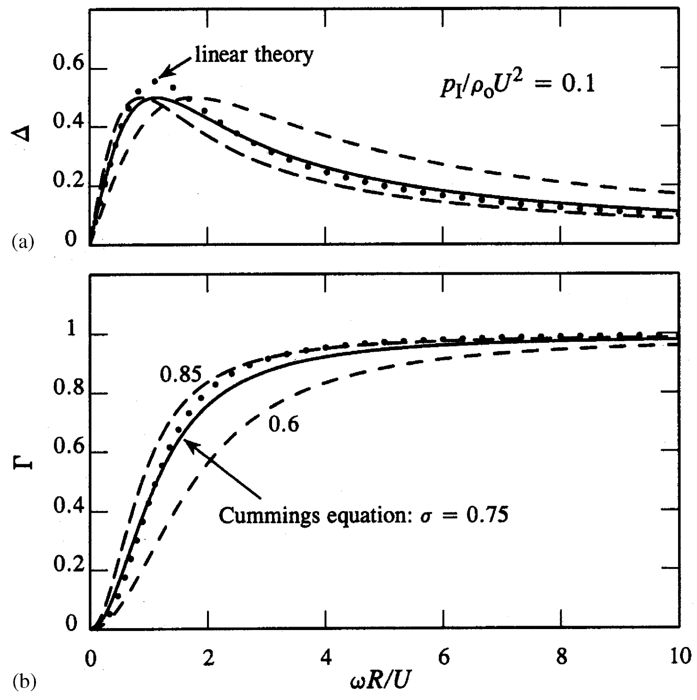

Figure 5. Comparison of $K_R/2R = \Gamma - \mathrm{i}\Delta$ determined by linear theory (...) and by the Cummings equation for $p_I/\rho_o U^2 = 0.1$ and $\sigma = 0.6, 0.75, 0.85$.

These limits coincide provided that $\sigma = \sqrt{2/\pi} \approx 0.8$, which again is close to the empirical value of σ recommended by Cummings (1986).

The terms $n \neq 1$ in the expansion (4.3) represent the nonlinear effects of flow through the aperture. However, the coefficient Δ and Eq. (2.4) (with $p_+ - p_- = p_I$) still determine the energy dissipated (the work done) by the pressure p_I in generating vorticity in the aperture. None of the coefficients V_n for $n \neq 1$ contributes to this dissipation. A detailed examination of the numerical solutions for $p_I/\rho_o U^2$ as large as 1 indicates that V_n is small for $n \geqslant 2$ and becomes negligible when $\omega R/U > 1$. The coefficient V_0 is real and *negative* for $\omega R/U \neq 0$, and represents a reduction in the mean volume flux produced by the unsteady pressure, but the effect is small except possibly at very low frequencies, as indicated in Fig. 6. The behaviour as $\omega R/U \to 0$ is nonuniform, because a *steady* additional applied pressure p_I actually increases the flux through the aperture.

4.3. Effect of amplitude on dissipation

The plots in Fig. 7 are evaluated from Eqs. (4.5) using the numerical solutions for the two extreme cases $p_I/\rho_o U^2 = 0.1$, 1.0. They indicate that the influence of amplitude on the damping of the incident pressure field is negligible. Indeed, the solution

$$V(t) = \frac{2p_I}{\pi \rho_o U} \frac{[(\omega R/U)\ \sin \omega t + (2/\pi\sigma^2)\ \cos \omega t]}{[(\omega R/U)^2 + (2/\pi\sigma^2)^2]} \tag{4.7}$$

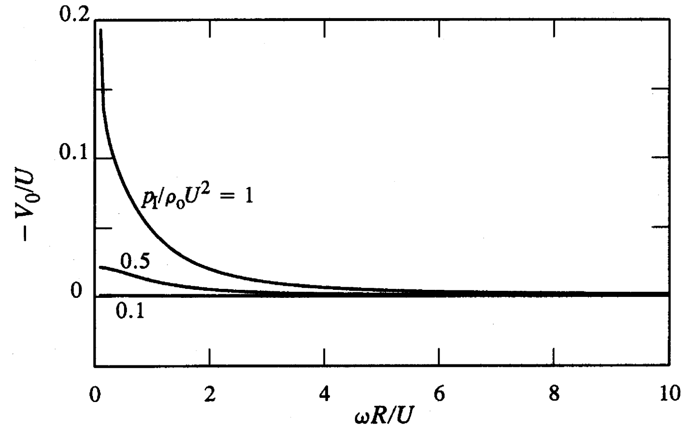

Figure 6. The mean flow coefficient V_0 in the expansion (4.3) of the solution of Cummings equation for $p_I/\rho_o U^2 = 0.1$, 0.5, 1.0.

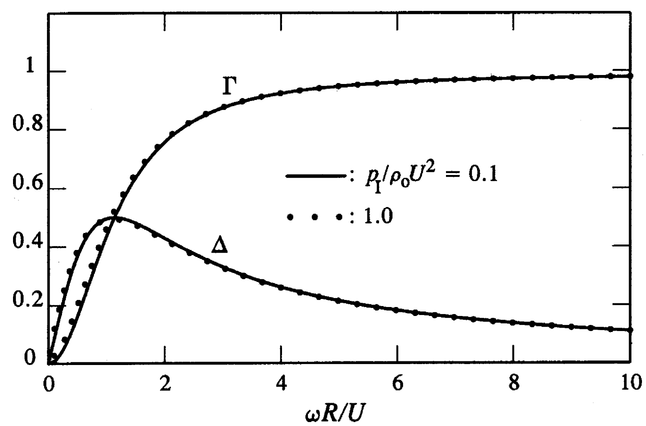

Figure 7. $K_R/2R = \Gamma - i\Delta$ determined by the Cummings equation for $p_I/\rho_o U^2 = 0.1$, 1.0.

of the *linearized* form of the Cummings equation (4.1) (obtained by deleting the term $V/2$ from the second term on the left-hand side) yields

$$\Gamma - \mathrm{i}\Delta = \frac{\omega R/U}{\omega R/U + 2\mathrm{i}/\pi\sigma^2}. \tag{4.8}$$

The frequency dependances of Γ and Δ predicted by this simple formula coincide with those represented by the solid curves in Fig. 7 for $p_I/\rho_o U^2 = 0.1$.

5. Conclusion

The attenuation of sound by vorticity production at surfaces and edges is greatly enhanced when a mean flow is present to sweep away vorticity energized by the sound. The linear theory of attenuation in a bias flow aperture in a thin wall agrees well with experiment. Linear and nonlinear estimates of dissipation are consistent over an order of magnitude variation in the amplitude of the perturbation pressure, up to levels approaching in magnitude that required to maintain the mean flow through the aperture. In both the linear and nonlinear regimes the bias flow conductivity for a thin wall ($\ell_w = 0$) is well approximated by the simple formula

$$K_R = 2R\left(\frac{\omega R/U}{\omega R/U + 2\mathrm{i}/\pi\sigma^2}\right), \tag{5.1}$$

where U is the mean velocity in the plane of the aperture and the contraction ratio $\sigma \approx 0.75$. This provides a useful alternative to the more complicated linear theory approximation (2.3) of Howe (1979,1998). The principal effect of nonlinearity is a small reduction in the mean bias flow velocity (typically less than about 5%).

The approximate agreement between the Cummings-equation formula (5.1), for which vortex shedding occurs in a jet with contraction ratio $\sigma < 1$, and the linear theory model (2.3) for which the shed vorticity is convected away without contraction can, perhaps, be explained as follows. Predictions at high frequencies are the same because phase interference between the influence of successive shed ‘vortex rings’ implies that the motion in the aperture is affected only by vortices close to the aperture, before significant contraction has occurred. The agreement at low frequencies is more approximate and is achieved by suitable adjustment of the effective contraction ratio σ in the Cummings equation.

Cummings’ equation (4.3) applied to a wall of finite thickness ($\ell_w > 0$) also indicates that nonlinearity has a negligible influence on the conductivity when flow reversal does not occur, in which case

$$K_R = \frac{K_o(\omega\ell/U)}{(\omega\ell/U) + \mathrm{i}/\sigma^2}, \quad \text{where } K_o = \frac{\pi R^2}{\ell}, \ \ \ell = \frac{\pi R}{2} + \ell_w. \tag{5.2}$$

This conclusion is qualitatively consistent with the linearized numerical investigation of Jing and Sun (1999), but it has not yet been validated experimentally.

Apart from the relevance of this formula to noise control engineering, it also has important applications to estimating acoustic losses and the corresponding broadening of resonance bandwidths in the human vocal tract. It can be used, for example, to quantify acoustic losses in the larynx, where pulses of air create the voice source. Voice pulses often occur at a relatively slow, ‘quasi-steady’ rate of 120 Hz for an adult male voice, and the maximum flow speed through the glottis during phonation can approach 30–40 m/s; for a good portion of the glottal pulse the slowly varying mean flow speed is therefore very much greater than the acoustic particle velocity (which does not exceed $\sim$1 m/s in voiced speech). In particular the results of this paper confirm and sharpen earlier estimates of bias flow losses in the vocal tract (Fant, 1970). Thus, it can be shown that Fant’s (1970, p. 269) approximation $\rho U/\pi R^2$ for the ‘differential resistance’ R_d of acoustic waves in the vocal tract produced by jet flows should take the modified and enhanced value $R_d \sim \rho U/\sigma^2 \pi R^2$ consistent with the Cummings equation.

References

Bechert, D., Michel, U., Pfizenmaier, E., 1977. Experiments on the transmission of sound through jets. American Institute of Aeronautics and Astronautics Paper 77-1278.

Birkhoff, G., Zarantonello, E.H., 1957. Jets, Wakes and Cavities. Academic Press, New York.

Cummings, A., 1984. Acoustic nonlinearities and power losses at orifices. American Institute of Aeronautics and Astronautics Journal 22, 786–792.

Cummings, A., 1986. Transient and multiple frequency sound transmission through perforated plates at high amplitude. Journal of the Acoustical Society of America 79, 942–951.
Dean, P.D., Tester, B.J., 1975. Duct wall impedance control as an advanced concept for acoustic suppression. NASA Contractor Report—134998.
Dowling, A.P., Hughes, I.J., 1992. Sound absorption by a screen with a regular array of slits. Journal of Sound and Vibration 156, 387–405.
Dupere, I.D.J., Dowling, A.P., 2000. Absorption of sound near abrupt area expansions. American Institute of Aeronautics and Astronautics Journal 38, 193–202.
Eldredge, J.D., Dowling, A.P., 2003. The absorption of axial acoustic waves by a perforated liner with bias flow. Journal of Fluid Mechanics 485, 307–336.
Fant, G., 1970. Acoustic Theory of Speech Production. Mouton, The Hague.
Howe, M.S., 1979. On the theory of unsteady high Reynolds number flow through a circular aperture. Proceedings of the Royal Society of London A 366, 205–233.
Howe, M.S., 1980. The dissipation of sound at an edge. Journal of Sound and Vibration 70, 407–411.
Howe, M.S., 1998. Acoustics of Fluid-structure Interactions. Cambridge University Press, Cambridge.
Hughes, I.J., Dowling, A.P., 1990. The absorption of sound by perforated linings. Journal of Fluid Mechanics 218, 299–336.
Jing, X., Sun, X., 1999. Effect of plate thickness on impedance of perforated plates with bias flow. American Institute of Aeronautics and Astronautics Paper 99-1877.
Jing, X., Sun, X., 2002. High-intensity sound absorption at an orifice with bias flow. Journal of Propulsion and Power 18, 718–720.
Lamb, H., 1932. Hydrodynamics, sixth ed. Cambridge University Press, Cambridge.
Melling, T.H., 1973. The acoustic impedance of perforates at medium and high sound pressure levels. Journal of Sound and Vibration 29, 1–65.
Rayleigh, L., 1945. Theory of Sound, vol. 2. Dover, New York.
Ver, I.L., 1982. Perforated baffles prevent flow-induced acoustic resonance in heat exchangers. Paper Presented at the 1982 Meeting of the Federation of the Acoustical Societies of Europe, Göttingen, September 1982.
Ver, I.L., 1990. Practical examples of noise and vibration control: case history of consulting projects. Noise Control Engineering Journal 35, 115–125.
Zinn, B.T., 1970. A theoretical study of nonlinear damping by Helmholtz resonators. Journal of Sound and Vibration 13, 347–356.